Published in final edited form as:
Nano Lett. 2010 January ; 10(1): 305–312. doi:10.1021/nl9035753.

Potato virus X as a novel platform for potential biomedical applications

Nicole F. Steinmetz[†,Π], **Marianne E. Mertens**[†,Δ], **Rebecca E. Taurog**[‡], **John E. Johnson**[‡], **Ulrich Commandeur**[Δ], **Rainer Fischer**[Δ,¥,*], and **Marianne Manchester**[†,Π,*]

Rainer Fischer: fischer@molbiotech.rwth-aachen.de; Marianne Manchester: marim@scripps.edu

[†] Department of Cell Biology, The Scripps Research Institute, 10550 North Torrey Pines Road, La Jolla, CA 92037, USA

[Π] Center of Integrative Molecular Biosciences, The Scripps Research Institute, 10550 North Torrey Pines Road, La Jolla, CA 92037, USA

[‡] Department of Molecular Biology, The Scripps Research Institute, 10550 North Torrey Pines Road, La Jolla, CA 92037, USA

[Δ] Institute for Biology VII, Department of Molecular Biotechnology, RWTH Aachen University, Worringer Weg 1

[¥] Fraunhofer Institute for Molecular Biology and Applied Ecology, Forckenbeckstrasse 6, 52074 Aachen, Germany

Abstract

We demonstrate that nanoparticles formed from the rod-shaped plant virus *Potato virus X* (PVX) can serve as a novel platform for biomedical applications. Bioconjugation protocols including amine modification and “click” chemistry allowed the efficient functionalization of PVX with biotins, dyes, and PEGs. Fluorescent-labeled and PEGylated PVX particles revealed that different fluorescent labels have a profound effect on PVX–cell interactions. Applying bioconjugation chemistries to PVX opens the door for chemical functionalization with targeting and therapeutic molecules.

Many novel nanomaterials have recently been developed for potential biomedical applications, each with advantages and disadvantages in terms of biocompatibility, bioavailability, pharmacokinetics, immunogenicity, and toxicity. Synthetic nanoparticles such as carbon nanotubes and quantum dots are often toxic and non-biodegradable, leading to persistent and undesirable side effects *in vitro* and *in vivo*.[1–3] In contrast, biological nanomaterials such as DNA, protein cages and viral nanoparticles (VNPs) are biocompatible, biodegradable and non-toxic. A broad range of VNPs has been developed. For example, the icosahedral particles of *Cowpea mosaic virus* (CPMV) and *Cowpea chlorotic mottle virus* (CCMV) have been extensively studied for both materials science and biomedical applications, as previously reviewed in [4, 5, 6], whereas rod-shaped VNPs such as *Tobacco mosaic virus* (TMV) and bacteriophage M13, have been utilized as nanotubes for batteries and nanowires. The potential of the archaeal virus *Sulfolobus islandicus* rod-shaped virus 2 (SIRV2) to serve as a template for bioconjugation chemistry has also been verified.[7–9]

[*]To whom correspondence should be addressed: fischer@molbiotech.rwth-aachen.de, Tel: +49-241-6085-11021, Fax: +49-241-6085-11025; marim@scripps.edu, Tel: +1-858-784-8086, Fax: +1-858-784-7979.

Supporting Information Available. Experimental details and supporting data. This information is available free of charge via the Internet at http://pubs.acs.org.

We have focused on the design of plant VNPs for biomedical applications such as targeted drug delivery and imaging. When developing novel nanomaterials for such purposes, the dimensions and surface characteristics of the particles must be considered as these will greatly influence *in vivo* properties such as biodistribution, plasma clearance, diffusion and penetration. Smaller particles penetrate tissue efficiently but are cleared more rapidly, whereas larger particles can avoid reticoendothelial clearance allowing them to accumulate in the target tissue, albeit at the expense of reduced permeability.[10] In terms of developing formulations specifically targeted to molecular receptors, rod-shaped particles are beneficial because they have a much larger surface area than spherical particles, thus offering more potential acceptor sites for functionalization with molecules used for imaging, targeting or therapeutic activity. For example, up to 240 fluorescent labels can be installed on a 30-nm diameter icosahedral CPMV particle[11], whereas more than 2000 dye molecules can be attached to the TMV particle[12], which is 300 nm long and 18 nm wide. As well as providing more acceptor sites, rod shaped particles also present the ligands in a more efficient manner. Cells are typically 10–100 times larger than a nanostructure and the cell surface tends to be flat. A rod-shaped particle may in theory interact with a larger number of binding sites on the cell surface, thus increasing targeting sensitivity and specificity.

Although the potential biomedical applications of a number of icosahedral VNP platforms have been studied in detail [4], the potential of rod-shaped VNPs has received comparatively little attention. We evaluated the properties of VNPs derived from the rod-shaped plant virus *Potato virus X* (PVX), specifically as a nanoparticle platform for biomedical applications. PVX is the type member of the Potexvirus group.[13] The particles are flexible rods 515 nm long and 13 nm wide, consisting of 1270 identical 25-kDa coat protein (CP) subunits. Natural PVX hosts are members of the family *Solanacea*, and *Nicotiana benthamiana* plants are also susceptible to mechanical inoculation, producing milligram quantities of particles from 1 g of infected leaf material. Infectious cDNA clones of PVX genomic RNA are available and genetic modification protocols have been established.[14] These methods allow PVX to be used for epitope presentation approaches in vaccine development. [15–17] Chimeric PVX particles have also been combined with enzymes for the fabrication of novel biocatalysts. [18] Whereas genetic modification procedures are well established, chemical bioconjugation methods have not yet been applied to PVX.

In order to make use of PVX for biomedical or other materials applications it is essential to establish chemical bioconjugation procedures. The crystal structure of PVX has not been solved, so it is unknown which amino acids are exposed on the surface of the particle and are available for chemical functionalization. Amino acids that can be easily modified using standard procedures and commercially available compounds include Lys (side chain amine groups) and Asp and Glu residues (carboxylate groups). Each of the 25-kDa PVX CP subunits (NCBI AAV27212) contains 11 Lys residues, 10 Asp residues and 10 Glu residues, which are potential targets for bioconjugation strategies. The CP of some strains of PVX is glycosylated, and carbohydrates are feasible candidates for chemical modification methods.[19, 20] The impact of our results on the development of PVX for potential biomedical applications is discussed.

The potential of PVX particles to accept functionalization was tested using three different chemistries. In an initial proof-of-principle study, particles were exposed to biotin with functional modifications representing three different coupling reactions, and modified particles were detected using streptavidin probes. First, biotin *N*-hydroxysuccinimide (NHS) esters were used to probe for reactive amine groups, where NHS ester-based amine coupling would result in the formation of a stable amide bond. Second, an amine-containing biotin-hydrazide was used in combination with the coupling reagents NHS and a 1-ethyl-3-(3-dimethylaminopropyl) carbodiimide (EDC) to probe for reactive carboxylic acid groups. EDC activates carboxylates via the formation of an *O*-acylisourea intermediate that readily reacts with amines to also form

a stable amide bond. Third, the addressability of glycans on the PVX coat protein was tested by subjecting carbohydrates to mild oxidation using sodium meta-periodate to convert primary hydroxyls into aldehydes, which are reactive toward biotin-hydrazide, forming a covalent hydrazone linkage. In all three reactions, activated biotin probes were used in a molar excess (10 for each CP) and the reaction was allowed to proceed overnight to ensure maximum labeling (Supporting Information). Samples were analyzed by denaturing polyacrylamide gel electrophoresis followed by western blots that were probed with streptavidin-alkaline phosphatase conjugates. Successful and efficient biotinylation was confirmed when biotin NHS esters were used to test for coupling to amines, but no biotinylation was observed with carboxylate-selective or carbohydrate-selective conjugation methods (Supporting Figure 1). This indicates that the PVX carboxylates are not solvent-exposed or are not accessible for the chemistry we used. Whether or not a specific residue can be utilized in bioconjugation depends on i) the exposure of that group to the solvent, and ii) the microenvironment. The finding that mild oxidation and subsequent reaction with biotin-hydrazide did not yield biotinylated PVX particles could also indicate that the strain (PV-0018 from the German Collection of Microorganisms and Cell Cultures; DSMZ) we used is not glycosylated.

We investigated the amine-based conjugation reaction in greater detail, studying the integrity of the labeled PVX particles and the number of labels that were displayed on the surface. This was achieved using the fluorescent label OregonGreen 488 (O488) NHS ester (Scheme 1), which was incubated either for 2 h or overnight with the PVX particles in increasing molar ratios (giving a molar excess label:CP of 1:1, 2:1, 5:1, 10:1 and 50:1, see Supporting information). The reaction mixture was purified using size exclusion centrifugal devices with a molecular weight cut-off of 10 kDa, and the columns were washed until the fluorescent dye was no longer detectable in the flow-through. The coupling reaction was essentially complete after 2 h. The number of O488 molecules per virion was determined by UV/visible spectroscopy (Figure 1). At a 10:1 molar excess of O488 over CP, PVX particles contained 1140 labels after 2 h, and 1146 labels following an overnight reaction. A 50% increase in efficiency could be achieved by increasing the molar excess of O488 over CP to 50:1, resulting in the detection of up to 1670 labels per PVX particle indicating that more than one Lys side chain per CP may be modified. Particle integrity for each sample was confirmed using a combination of native and denaturing gel electrophoresis, size exclusion chromatography and transmission electron microscopy (see below).

We next explored the feasibility of using more advanced conjugation chemistries such as Cu (I)-catalyzed azide-alkyne 1,3-dipolar cycloaddition (CuCAAC) reactions ("click" chemistry). Click reactions have been widely used for bioconjugation and are a popular strategy because of their specificity, high yield and the wide range of solvents and pH stabilities.[21] Click chemistry protocols have been established for VNPs and broad classes of molecules ranging from small chemical modifiers to intact proteins have been covalently attached to VNPs such as CPMV, bacteriophage Q β, and TMV using this method.[22–25] In order to use click chemistry on PVX, an alkyne group was installed as an acceptor site on Lys side chains using *N*-(4-pentynoyloxy) succinimide (Scheme 1) (Coupling methods are described in the Supporting Information). To quantify the number of free alkynes per PVX particle, we adopted a previously-reported fluorescence assay based on coumarin compounds.[26] Briefly, non-fluorescent 3-azidocoumarin was added to PVX-alkyne under click conditions (Supporting Information). Coupling of the non-fluorescent 3-azidocoumarin to an alkyne leads to the formation of a fluorescent triazolylcoumarin moiety, whose absorbance can be followed at 475 nm. A known concentration of propargyl alcohol was used as an internal standard allowing free alkynes to be quantified, revealing the presence of approximately 110 alkynes per PVX particle. Approximately 10% of the CPs were labeled with an alkyne.

To confirm that alkyne groups can be utilized to install functionalities and to verify that the particles remain intact under the necessary reaction conditions, an azide-activated fluorescein (5-carboxamido-(3-azidopropyl) fluorescein)) was conjugated to alkyne-substituted PVX particles under click conditions (Supporting Information)[23] to give PVX-fluorescein. Samples were purified and then analyzed by native (not shown) and denaturing gel electrophoresis, SEC and TEM (Figure 2). Denaturing gel electrophoresis confirmed the covalent attachment of fluorescein to the CP as indicated by the appearance of a fluorescent band under UV light (Figure 2A). Particle integrity was confirmed by SEC using Superose-6, where the native and modified particles had a similar elution profile (Figure 2B). The absorbance ratio at 260/280 nm was 1.22 for native particles and 1.26 for PVX-fluorescein, providing further evidence of particle integrity. When a third laser was set to 496 nm (the absorbance maximum of fluorescein), the fluorescent dye co-eluted with PVX confirming its covalent attachment. TEM studies also verified that the particles were intact (Figure 2C), since aggregates and particle fragments were not observed. UV/visible spectroscopy using the specific extinction coefficient of fluorescein (70,000 cm^{-1} M^{-1} at a wavelength of 496 nm) showed that particles contained 100 fluorescein moieties, indicating that basically all of the installed alkynes were utilized in the click reactions and coupled to fluorescein-azide.

With bioconjugation methods successfully established for PVX, we next studied how PVX and polyethylene glycol (PEG)-conjugated PVX interacted with two mammalian cells lines – HeLa (human cervical cancer cell line) and BalbCl7 (mouse fibroblast cell line). Various PVX-dye and PVX-dye-PEG conjugates were designed and evaluated, and particles were labeled with either O488 or AlexaFluor 647 (A647) using activated NHS esters. PEG1000 and PEG2000 were used as activated NHS esters (Scheme 1). We chose two different PEGs with different chain lengths because we have previously found that the shielding efficiency of PEGylated CPMV particles is highly dependent on the chain length and the surface grafting area effectively covered by the PEG chains.[27] The following particle formulations were prepared: PVX-O488, PVX-A647, P1 (= PVX-PEG1000), P2 (= PVX-PEG2000), P1-O488, P2-O488, and P2-A647. In order to generate the double-labeled formulations, the fluorophores and PEGs were each provided at a molar excess of 5:1 over the CP, and the reaction was carried out for 2 h prior to purification by ultracentrifugation to remove excess chemicals.

The resulting hybrid VNPs were characterized using a combination of biochemical methods. All particle constructs were analyzed by denaturing gel electrophoresis, SEC and TEM (Figure 2, Supporting Figures 2 and 3), and UV/visible spectroscopy (Supporting Figure 4). Denaturing gels confirmed covalent attachment of the fluorescent dyes O488 (visualized under UV light) and A647 (under white light). Mobility shifts in the bands representing PEGylated CP subunits also confirmed successful PEGylation of the particles (Figure 2A). SEC and TEM verified the integrity of the virions. Elution profiles and the 260/280 nm absorbance ratio agreed with values obtained for native PVX virions, and the fluorophore co-eluted with the five fluorescently-labeled virions (Figure 2B). TEM data were consistent with the presence of intact VNPs with an average length of ~500 nm (Figure 2C, Supporting Figure 3).

Two different methods were used to determine labeling efficiency in these experiments: UV/visible spectroscopy to determine the number of fluorescent labels per particle (Supporting Figure 4) and the comparison of band intensities (non-labeled vs. PEGylated CP bands) after Safestain Blue staining using FluorChemSP software in the case of PEG-labeled particles.[27] The results, summarized in Table 1, show that 70–90% of the CPs were labeled when an excess of 10 fluorophores per CP was provided, whereas this fell to 25–40% in the double-labeled particles because of the lower molar excess. Whereas dye-conjugation yielded fully decorated particles (i.e. nearly every subunit was modified with a fluorescent label), only partial labeling was observed when conjugating large PEG polymers. Only 20% of CPs were labeled with PEG1000 and 40% with PEG2000, and these efficiencies halved when applying the double-

labeling strategy. The higher-density labeling with the longer polymer, PEG2000, may reflect the fact that longer polymers are more hydrophilic, which should benefit the coupling reaction. At least two independent experiments were carried out to confirm reproducibility.

Next we investigated the interaction between the fluorescent-labeled and PEGylated PVX particles (PVX-O488, P1-488 and P2-488; PVX-A647 and P2-A647) and the HeLa and BalbCl7 cells described above. Qualitative data were obtained by confocal microscopy (Figures 3 and 4) and quantitative data by flow cytometry (Figure 5). We found that the fluorescent-labeled particles PVX-O488 and PVX-A647 were able to interact with both HeLa and BalbCl7 cells, interactions with the latter cells being strongest (Figures 3 and 5). Cellular interactions can be advantageous when developing therapeutic probes for tumor delivery by making use of enhanced permeability and retention (EPR) effects. For effective treatment cellular delivery is desired. These strategies have been developed and work effectively for rods such as single-walled carbon nanotubes (SWCNTs).[28] Based on the similar dimensions and aspect ratio of PVX and SWCNTs, we expect that these strategies can also be adapted for PVX particles.

The PVX-A647 formulation was chosen to gain further insights into PVX-cell interactions, specifically whether PVX particles were bound onto the cell surface or internalized. Native PVX particles were used as a negative control (Figure 4A), and O488-labeled CPMV particles (Supporting Information) were used as a positive control. CPMV-cell interactions are well understood and CPMV is known to be internalized by cells.[29] Confocal microscopy showed that PVX-A647 and CPMV-O488 particles were at least in part co-localized in HeLa cells (Figure 4D) indicating that PVX is internalized rather than bound to the cell surface.

Cellular uptake was further confirmed by cell-surface staining using A555-labeled wheat germ agglutinin (WGA-A555), which stains the glycocalyx,[30] and recording Z-dimensional data. Analysis of Z-sections using ImageJ or Imaris software confirmed the internalization of PVX-A647 particles and their accumulation close to the nucleus (Figure 4B–C, E–I). Future studies will include co-localization immunostaining of intracellular organelles such as endosomes, lysosomes, and the endoplasmatic reticulum. Co-localization studies may give further clues about the trafficking and fate of PVX within the cell.

To determine the internalization time course, PVX-A647 particles were added to HeLa cells growing in medium, and the cells were washed and subsequently fixed at 0, 10, 60, 180 and 360 min post incubation. No particles were detected in cells freshly supplemented with PVX-A647 (time point 0 min). PVX-A647 particles were detected bound to the cell surface after 10 min and were found to be internalized after 60 min, with diffuse intracellular localization. Longer incubation times allowed the particles to accumulate in the peri-nuclear compartment. There were no apparent differences between cells observed 180 and 360 min post incubation (Figure 4J).

Next we set out to determine whether PEGylation reduces or shields cellular interactions. PEGylation is frequently used for the formulation of pharmaceuticals because it reduces biospecific interactions, increases solubility and stability, improves pharmacokinetics, reduces renal clearance, and reduces immunogenicity.[31–33]

First, we investigated the threshold number of particles per cell to render a positive signal by flow cytometry. Dye-labeled and PEGylated PVX samples at concentrations ranging from 10^3 to 10^5 PVX particles per cell were incubated with HeLa and BalbC17 cells. Although 10^4 PVX particles per cell rendered a weak positive signal, a significant signal was achieved when using 10^5 particles per cell (Figure 5C and Table S1 in Supporting Information), agreeing with results from other VNP platforms such as CPMV.

PEGylation generally reduces cellular interactions for CPMV and TMV particles.[12, 27, 34] However, the effects of PEGylation on PVX were somewhat contradictory. PVX particles labeled with both PEG and O488 interacted less efficiently with cells than non-PEGylated O488- labeled PVX, which is consistent with our studies PEGylating CPMV particles.[27] Also, when comparing the shielding efficiency of P1-O488 and P2-O488, our observations are in accordance with previous reports[27] showing that longer PEGs with a larger surface grafting area confer better shielding effects. P1-O488 reduced PVX-cell interactions by 30% for HeLa cells and by 70% in the case of BalbC17 cells, whereas P2-O488 effectively blocked the interaction, reducing it by 60% and 80%, respectively (Figure 5, and Table S1 in the Supporting Information). Interestingly, A647-labeled PVX generated the opposite result: the PEGylated particle formulation P2-A647 interacted more efficiently with cells than non-PEGylated PVX-A647. This was true for both cell lines, and was consistent with confocal imaging and flow cytometry data (Figures 3 and 5, and Table S1 in the Supporting Information).

P2-O488 effectively shields PVX from its interaction with cells, whereas P2-A647 positively encourages the interaction. Both particle formulations were shown to be intact and lacked aggregates, as indicated by native gel electrophoresis (not shown), SEC, and TEM (Figure 2B, C). The particles were also labeled to a similar degree, P2-O488 with 390 fluorophores (30% of CPs) and 300 PEG chains (25% of CPs), P2-A647 with 440 fluorophores (35% of CPs) and 380 PEG moieties (30% of CPs) (Table 1). These data suggest that the A647 dye alters the biophysical and *in vitro* properties of the labeled particles in such a way that, when combined with PEG, higher cellular uptake is promoted along with the loss of any shielding effects.

O488 is a rather small molecule with a molecular weight of ~500 Da, and the ring structure (Scheme 1) can be regarded as relatively hydrophobic. The structure of A647 is still considered proprietary, but its molecular weight is ~1300 Da, which makes it 2.6 times larger than O488, and it is expected to be even more hydrophobic. There have been no reports describing the effects of A647 on particle–cell interactions, and our data indicate that the dye influences the *in vitro* properties of PEGylated PVX. Similarly contradictory observations have been made in previous reports studying PEGylated SWCNTs. For example, PEGylated SWCNTs do not interact with cells, [35, 36] but SWCNTs displaying both PEG and fluorescein do interact with cells and the material accumulates in the nucleus.[37, 38] The fact that the fluorescent labels can alter the biophysical or *in vitro* properties of a nanomaterial is a significant observation and underscores the importance of carefully designing each formulation.

To understand the biophysical differences between P1-O488, P2-O488 and P2-A647 we modeled the conformation of each PEG and the theoretical surface grafting area, i.e. the area that is effectively shielded. PEG chains can exist in either a condensed, mushroom-like conformation or a stretched-out, brush-like conformation. According to de Gennes, the conformation can be estimated based on the distance (D) between two adjacent PEG chains relative to their Flory dimension (R_F), the latter being related to the chain length.[33,39–41] A brush-like conformation appears when $D < R_F$, the chains fold into a mushroom-like conformation when $D > R_F$, and intermediate structures are observed when $D \sim R_F$.[40]

The X-ray structure of PVX has yet to be solved, so the Lys residues that serve as anchoring points cannot be mapped onto the particle's structure. Based on labeling density (Table 1) and knowledge about the arrangement of the CPs in the viral helix, the distance between two PEG chains can be estimated, using a similar method to that previously described for PEGylated CPMV[27] (for details see Supporting information). We estimated that 0.5% of the surface area of P1-O488 is covered with PEG, whereas the coverage of P2-O647 is 1.3%, and that of P2-A647 is 1.6%. One must take into account that the flexible PEG chains potentially rotate around the attachment site on the virion and thus could occupy and block the surface area within that radius. It is intriguing that subtle differences in surface coverage values that are already very

low are sufficient to effectively shield the P2-O488 formulation. This observation agrees with a previous report on PEGylated CPMV particles, where we also found that while CPMV particle-cell interactions were reduced when PEG1000 was attached (surface coverage was ~0.5%), effective shielding could only be achieved using PEG2000, which provided 0.8% coverage.[27]

In summary, we have established chemical bioconjugation methods that allow the covalent modification of PVX CP subunits and the consequent display of functionalized molecules. Using a molar excess of 10 labels per CP, essentially all 1270 CPs can be functionalized using standard amine chemistries, and up to 1670 labels can be introduced under more robust labeling conditions. Amine-selective chemistries are feasible when attaching small chemical modifiers. However, for larger ligands, strongly hydrophobic and less soluble molecules, more efficient conjugation strategies such as click chemistry may be required to achieve efficient labeling, and we also showed that PVX particles remain intact under click reaction conditions.

We designed and fabricated various fluorescent-labeled and PEGylated PVX particles. PVX-cell interactions could be reduced or blocked when working with O488-labeled PEGylated formulations, but PEGylation had no shielding effect when applied to A647-labeled PVX particles. Instead of shielding, P2-A647 interacts more strongly with cells. These results indicate that the fluorescent label may have a significant impact on the biophysical properties of the particle formulation. This is a phenomenon previously reported for SWCNTs[37, 38], emphasizing that the consequences of combining multiple chemical components in a nanoparticle formulation must be evaluated carefully. We have demonstrated that PVX can be used as a novel nanoplatform for potential applications in biomedicine. Future studies will investigate the *in vivo* properties of PVX particles and how these can be exploited by chemical functionalization with targeting and therapeutic molecules.

Supplementary Material

Refer to Web version on PubMed Central for supplementary material.

Acknowledgments

This work was funded by an American Heart Association Postdoctoral Fellowship (to N.F.S), NIH grant 1K99EB009105 (to N.F.S), a student fellowship from the Bayer Science & Education Foundation (to M.E.M.), the German Academic Exchange Service (DAAD; to M.E.M.), NIH grant CA112075 (to M.M.), a Ruth L. Kirschstein National Research Service Award to R.E.T. (F32 GM-084476), and a grant from NIH/NIGMS to J.E.J. (GM-054076). Vu Hong (TSRI) is thanked for helpful discussions regarding click chemistry and providing reagents for click reactions.

References

1. Hardman R. Environ Health Perspect 2006;114(2):165–72. [PubMed: 16451849]
2. Prato M, Kostarelos K, Bianco A. Acc Chem Res 2008;41(1):60–8. [PubMed: 17867649]
3. Takagi A, Hirose A, Nishimura T, Fukumori N, Ogata A, Ohashi N, Kitajima S, Kanno J. J Toxicol Sci 2008;33(1):105–16. [PubMed: 18303189]
4. Manchester M, Singh P. Adv Drug Deliv Rev 2006;58(14):1505–22. [PubMed: 17118484]
5. Steinmetz NF, Lin T, Lomonossoff GP, Johnson JE. Curr Top Microbiol Immunol 2009;327:23–58. [PubMed: 19198569]
6. Young M, Willits D, Uchida M, Douglas T. Annu Rev Phytopathol 2008;46:361–84. [PubMed: 18473700]
7. Nam KT, Kim DW, Yoo PJ, Chiang CY, Meethong N, Hammond PT, Chiang YM, Belcher AM. Science 2006;312(5775):885–8. [PubMed: 16601154]
8. Steinmetz NF, Bize A, Findlay KC, Lomonossoff GP, Manchester M, Evans DJ, Prangishvili D. Adv Funct Mater 2008;18:3478–3486.

9. Tseng RJ, Tsai C, Ma L, Ouyang J, Ozkan CS, Yang Y. Nature Nanotechnology 2006;1:72–77.
10. Thurber GM, Schmidt MM, Wittrup KD. Adv Drug Deliv Rev 2008;60:1421–1434. [PubMed: 18541331]
11. Wang Q, Kaltgrad E, Lin T, Johnson JE, Finn MG. Chem Biol 2002;9(7):805–11. [PubMed: 12144924]
12. Schlick TL, Ding Z, Kovacs EW, Francis MB. J Am Chem Soc 2005;127:3718–3723. [PubMed: 15771505]
13. Koenig, R.; Lesemann, DE. Potato virus X, potexvirus group. Vol. 354. Association of Applied Biologists; Warwick: 1989. p. 1-5.
14. Baulcombe DC, Chapman S, Santa Cruz S. Plant J 1995;7(6):1045–53. [PubMed: 7599646]
15. Uhde K, Fischer R, Commandeur U. Arch Virol 2005;150(2):327–40. [PubMed: 15503224]
16. Uhde-Holzem K, Fischer R, Commandeur U. Arch Virol 2007;152(4):805–11. [PubMed: 17216135]
17. Yusibov V, Rabindran S, Commandeur U, Twyman RM, Fischer R. Drugs R D 2006;7(4):203–17. [PubMed: 16784246]
18. Carette N, Engelkamp H, Akpa E, Pierre SJ, Cameron NR, Christianen PC, Maan JC, Thies JC, Weberskirch R, Rowan AE, Nolte RJ, Michon T, Van Hest JC. Nat Nanotechnol 2007;2(4):226–9. [PubMed: 18654267]
19. Baratova LA, Fedorova NV, Dobrov EN, Lukashina EV, Kharlanov AN, Nasonov VV, Serebryakova MV, Kozlovsky SV, Zayakina OV, Rodionova NP. Eur J Biochem 2004;271(15):3136–45. [PubMed: 15265033]
20. Tozzini AC, Ek B, Palva ET, Hopp HE. Virology 1994;202(2):651–8. [PubMed: 8030230]
21. Kolb HC, Finn MG, Sharpless KB. Angew Chem Int Ed Engl 2001;40(11):2004–2021. [PubMed: 11433435]
22. Bruckman MA, Kaur G, Lee LA, Xie F, Sepulveda J, Breitenkamp R, Zhang X, Joralemon M, Russell TP, Emrick T, Wang Q. Chembiochem 2008;9(4):519–23. [PubMed: 18213566]
23. Sen Gupta S, Kuzelka J, Singh P, Lewis WG, Manchester M, Finn MG. Bioconjug Chem 2005;16 (6):1572–9. [PubMed: 16287257]
24. Sen Gupta S, Raja KS, Kaltgrad E, Strable E, Finn MG. Chem Commun (Camb) 2005;(34):4315–7. [PubMed: 16113733]
25. Wang Q, Chan TR, Hilgraf R, Fokin VV, Sharpless KB, Finn MG. J Am Chem Soc 2003;125(11): 3192–3. [PubMed: 12630856]
26. Sivakumar K, Xie F, Cash BM, Long S, Barnhill HN, Wang Q. Org Lett 2004;6(24):4603–6. [PubMed: 15548086]
27. Steinmetz NF, Manchester M. Biomacromolecules 2009;10(4):784–92. [PubMed: 19281149]
28. Liu Z, Chen K, Davis C, Sherlock S, Cao Q, Chen X, Dai H. Cancer Res 2008;68(16):6652–60. [PubMed: 18701489]
29. Lewis JD, Destito G, Zijlstra A, Gonzalez MJ, Quigley JP, Manchester M, Stuhlmann H. Nat Med 2006;12(3):354–60. [PubMed: 16501571]
30. Wright CS. J Mol Biol 1984;178(1):91–104. [PubMed: 6548265]
31. Harris JM, Chess RB. Nat Rev Drug Discov 2003;2(3):214–21. [PubMed: 12612647]
32. Roberts MJ, Bentley MD, Harris JM. Adv Drug Deliv Rev 2002;54(4):459–76. [PubMed: 12052709]
33. Wattendorf U, Merkle HP. J Pharm Sci. 2008
34. Raja KS, Wang Q, Gonzalez MJ, Manchester M, Johnson JE, Finn MG. Biomacromolecules 2003;3:472–6. [PubMed: 12741758]
35. Liu Z, Winters M, Holodniy M, Dai H. Angew Chem Int Ed Engl 2007;46(12):2023–7. [PubMed: 17290476]
36. Zeineldin R, Al-Haik M, Hudson LG. Nano Lett 2009;9(2):751–7. [PubMed: 19152309]
37. Cheng J, Fernando KA, Veca LM, Sun YP, Lamond AI, Lam YW, Cheng SH. ACS Nano 2008;2 (10):2085–94. [PubMed: 19206455]
38. Nakayama-Ratchford N, Bangsaruntip S, Sun X, Welsher K, Dai H. J Am Chem Soc 2007;129(9): 2448–9. [PubMed: 17284037]

39. Nicholas AR, Scott MJ, Kennedy NI, Jones MN. Biochim Biophys Acta 2000;1463(1):167–78. [PubMed: 10631306]

40. de Gennes PG. Adv Colloid Interface Sci 1987;27:189–209.

41. Svergun DI, Ekstrom F, Vandegriff KD, Malavalli A, Baker DA, Nilsson C, Winslow RM. Biophys J 2008;94(1):173–81. [PubMed: 17827244]

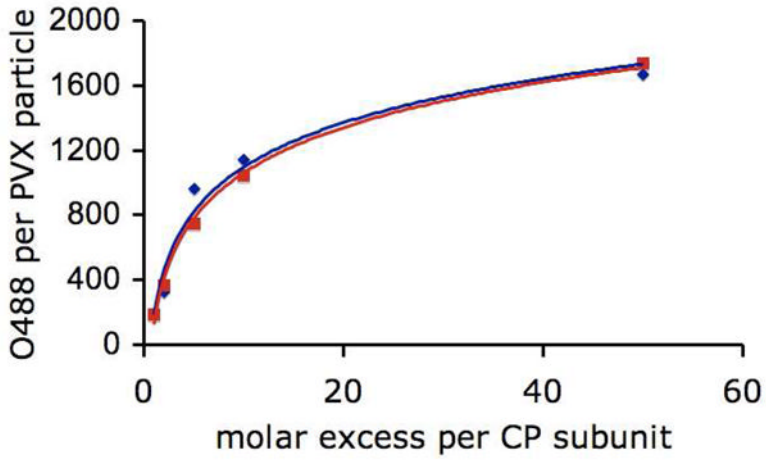

Figure 1.
Relationship between the excess of ligand used and the number of ligands attached per PVX particle. The number of O488 ligands per PVX particle was quantified by UV/visible spectroscopy and the O488 specific extinction coefficient (ε = 70,000 M^{-1} cm^{-1} at 496 nm). Red squares = overnight incubation, blue diamonds = 2 h incubation.

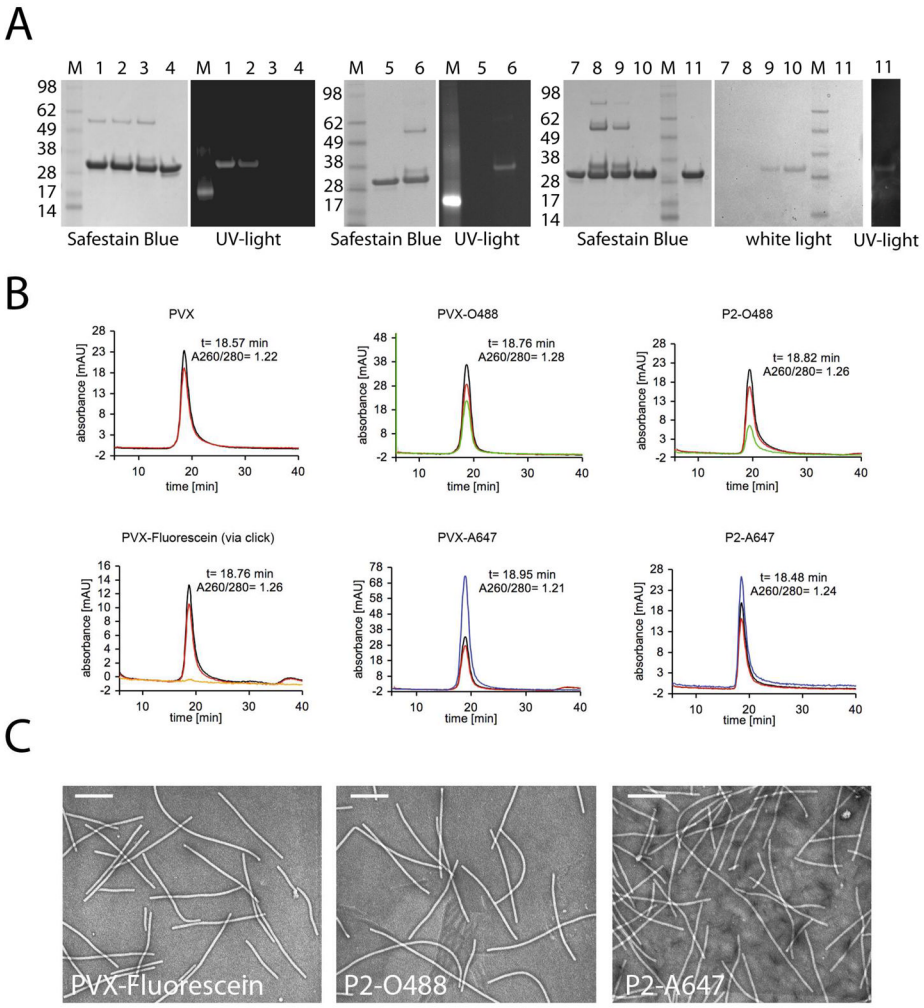

Figure 2.

Biochemical characterization of fluorescently-labeled and PEGylated PVX particles using denaturing gel electrophoresis (A), SEC (B), and TEM (C). A. 10 μg PVX samples were analyzed on 4–12% NuPage gels in 1x MES SDS buffer. Protein bands were visualized under UV light, white light, and after Safestain Blue staining. The molecular weight of the bands of the protein marker (M) are shown on the left in kDa. 1 = PVX-O488, 2 = P1-O488, 3 = P1, 4 = PVX, 5 = PVX, 6 = P2-O488 (loaded 6 μg), 7 = PVX (6 μg), 8 = P2, 9 = P2-A647, 10 = PVX-A647, 11 = PVX-Fluorescein. B. SEC using a Sepharose-6 column and ÄKTA Explorer. Samples were analyzed at a flow rate of 0.5 ml min^{-1}. Elution profiles per time (min) are provided. Laser settings: black line = 260 nm (RNA), red = 280 nm (protein), green and orange = 496 nm (O488 and fluorescein), blue = 650 nm (A647). The inset shows the time at elution peak and the ratio of A 260 nm:280 nm which is 1.22 for native particles. C. TEM micrographs of negatively stained (UAc) PVX particles. The scale bar is 200 nm. The magnification was 53,000x for all samples.

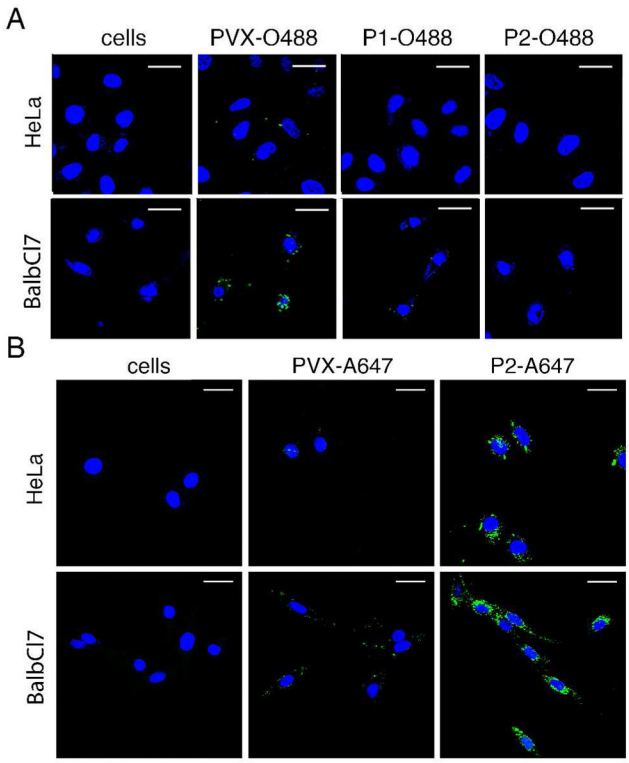

Figure 3.

Evaluating PVX-cell interactions using confocal microscopy. HeLa cells and BalbCl7 cells were probed with various fluorescent dye-labeled and PEGylated PVX formulations. Cell nuclei were stained with DAPI and are shown in blue. PVX is shown in green. Imaging was performed using a Biorad 2100 confocal microscope with a 60x oil objective. Data were analyzed and images were created using ImageJ. The scale bar is 30 μm.

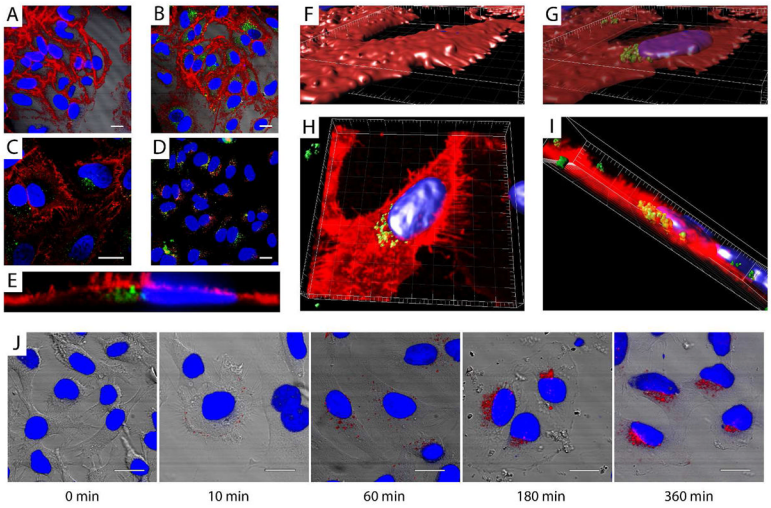

Figure 4.

Evaluating fluorescent-labeled PVX-cell interactions using HeLa cells and confocal microscopy. A. PVX particles (negative control). The cell membrane was stained with A555-labeled wheat germ agglutinin (WGA-A555, in red). A differential interference contrast (DIC) image is shown in the background of the fluorescent image. B. PVX-A647 (pseudocolored in green) and WGA-555 (in red), with DIC image in the background. C. PVX-A647 (in green) and WGA-555 (in red) (2x zoom). D. PVX-A647 (in green) and CPMV-O488 (in red). A–D. Images were analyzed using Image J. E.–I. Z-sections were recorded at a step size of 0.3 μm. PVX-A647 is shown in green and WGA-A555 staining is shown in red. E. Analysis of the data using ImageJ software, a cross-section through the cell is shown, the section comprises four frames and is 1.2 μm deep. F–I. Same cell as shown in Panel E. The data were analyzed using Imaris Software. F. WGA-A555 stain (cell membrane) is shown as solid. G. Side view, WGA-A555 (cell membrane) is shown transparent. H. Top view. I. Side view. J. Time course of PVX uptake. PVX-A647 is shown in red. A merge of the fluorescent images and DIC images is shown. A–J. Cell nuclei were stained with DAPI and are shown in blue. The scale bar is 20 μm in all images. 10^5 particles per cell were added to the cells. A–I. Incubation time was 3 h. J. Incubation time as noted. Imaging was performed using a Biorad 2100 confocal microscope with a 60x oil objective.

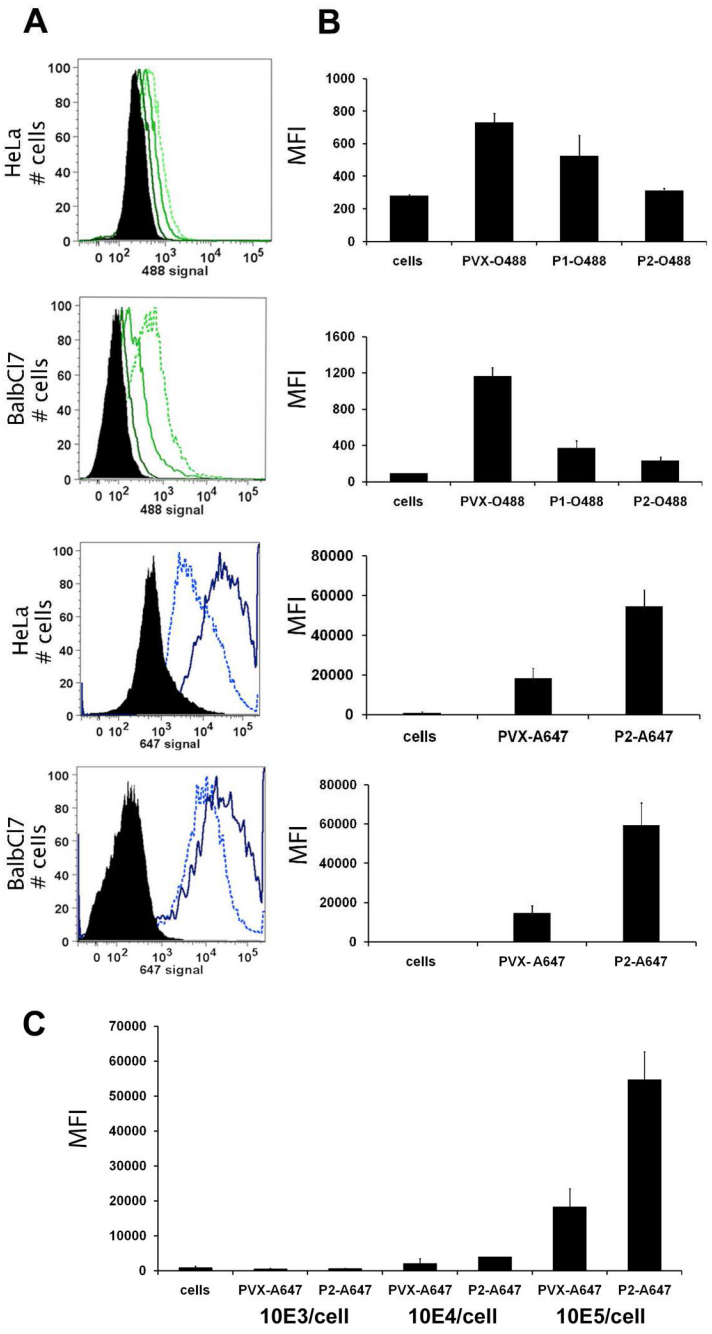

Figure 5.

Evaluating PVX–cell interactions using flow cytometry. HeLa cells and BalbCl7 cells were probed with various fluorescent dye-labeled and PEGylated PVX formulations. A. Histograms: black filled histogram = cells only, light green dotted histogram = PVX-O488, light green histogram = P1-O488, dark green histogram = P2-O488, light blue dotted histogram = PVX-A647, dark blue histogram = P2-A647. B. Statistical analysis using FlowJo software showing the mean fluorescence intensity (MFI) for each sample. Data are also summarized in Table S1 (see Supporting Information). Error bars indicate mean +/− S.D. C. PVX-A647–cell interactions were tested at varying particle/cell ratios to determine the threshold of particles needed to render a positive signal. Experiments were conducted using 10^3, 10^4, and 10^5 PVX

particles per cell. Experiments were repeated at least twice and triplicate samples were analyzed. 10,000 events were recorded.

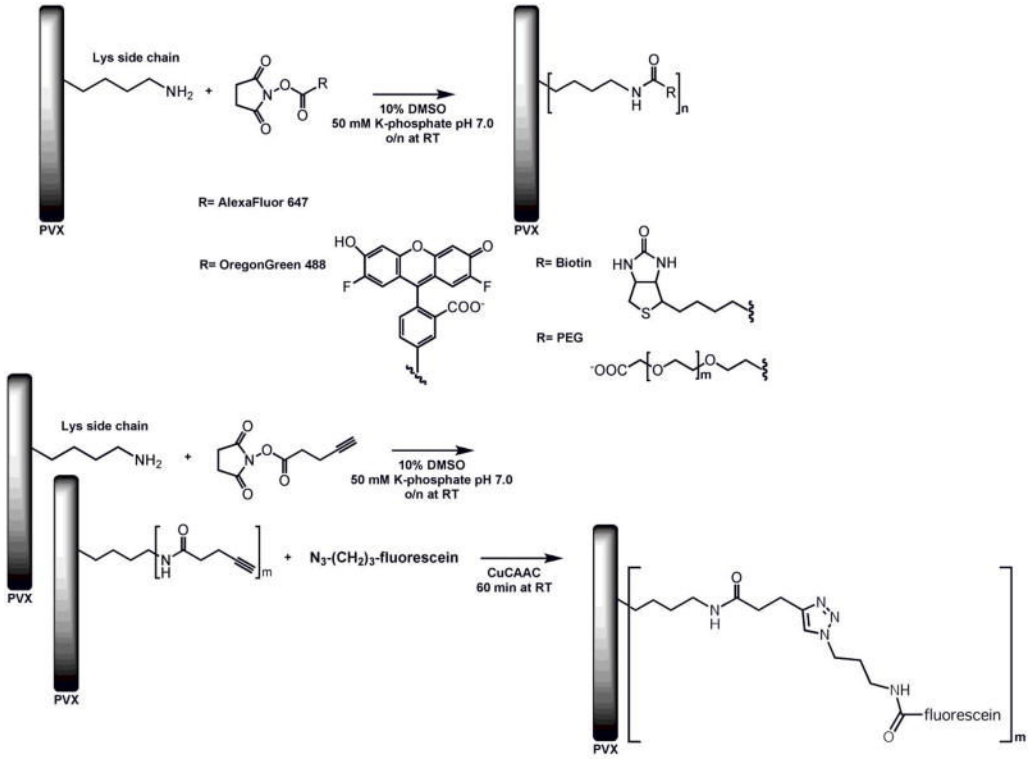

Scheme 1.

Chemical labeling of PVX with fluorescent dyes and PEG chains using NHS ester-based chemistries (A) or click reactions (B). CuCAAC = Cu(I)-catalyzed azide-alkyne cycloaddition.

Table 1

Number of fluorescent labels and PEG chains displayed per PVX particle formulation

PVX particle formulation	Approximate values of # dyes per PVX (% CPs labeled)	Approximate values of # PEGs per PVX (% CPs labeled)
PVX-O488	860 (70%)	NA
PVX-A647	1100 (90%)	NA
P1	NA	270 (20%)
P1-O488	520 (40%)	130 (10%)
P2-O488	390 (30%)	300 (25%)
P2	NA	510 (40%)
P2-A647	440 (35%)	380 (30%)